NASA-CR-204658

JOURNAL OF GEOPHYSICAL RESEARCH, VOL. 102, NO. A2, PAGES 2279-2289, FEBRUARY 1, 1997

Relative concentration of He^+ in the inner magnetosphere as observed by the DE 1 retarding ion mass spectrometer

P. D. Craven and D. L. Gallagher
Space Sciences Laboratory, NASA Marshall Space Flight Center, Huntsville, Alabama

R. H. Comfort
Center for Space Plasma and Aeronomic Research, University of Alabama in Huntsville, Huntsville

Abstract. With observations from the retarding ion mass spectrometer on the Dynamics Explorer 1 from 1981 through 1984, we examine the He^+ to H^+ density ratios as a function of altitude, latitude, season, local time, geomagnetic and solar activity. We find that the ratios are primarily a function of geocentric distance and the solar EUV input. The ratio of the densities, when plotted as a function of geocentric distance, decrease by an order of magnitude from 1 to 4.5 R_E. After the He^+ to H^+ density ratios are adjusted for the dependence on radial distance, they decrease nonlinearly by a factor of 5 as the solar EUV proxy varies from about 250 to about 70. When the mean variations with both these parameters are removed, the ratios appear to have no dependence on geomagnetic activity, and weak dependence on local time or season, geomagnetic latitude, and L shell.

Introduction

Solar EUV radiation at 304 Å which is resonantly scattered from He^+ has been proposed as a possible candidate for imaging of the magnetosphere [*Johnson et al.*, 1971; *Meier and Weller*, 1972; *Weller and Meier*, 1974; *Waite et al.*, 1984]. The spatial distribution of the He^+ density in the magnetosphere determines the amount of scattered 304 Å energy that reaches the detector from an element of solid angle along a given line of sight. Since the distribution of He^+ ions is considered to be optically thin, the energy reaching a detector is the sum of all the sources in the line of sight. Therefore some a priori knowledge of the average spatial and temporal distribution of the He^+ would be helpful in deconvolving images of the inner magnetosphere. Models that have been used to simulate a magnetosphere image from He^+ have approximated the spatial distribution by assuming a constant He^+ density, above some base altitude on a given L shell [*Meier and Weller*, 1972; *Weller and Meier*, 1974], or alternatively, a constant He+ to total denisity ratio; E. C. Roelof et al., unpublished manuscript, 1992], where total density in the magetosphere is assured to be represented by H+. *Williams et al.* [1992] noted that one of the important consequences of He^+ following the H^+ density is that images from He^+ resonance scattering then also represent the total plasma and not just He^+. The behavior of the He^+ to H^+ ratio will be important in models of the inner magnetosphere, in understanding the physics of the light ions, and in interpreting images of the magnetosphere obtained using scattered 304 Å radiation.

Observations from the retarding ion mass spectrometer (RIMS) on Dynamics Explorer 1 (DE 1) early in the lifetime of the satellite [*Horwitz et al.*, 1984; *Comfort et al.*, 1988], show the He^+ to H^+ density ratio to be of order 0.2 for the conditions experienced. *Newberry et al.* [1989] noted that the DE 1/RIMS He^+ to H^+ density ratios were higher than had previously been reported [*Chappell et al.*, 1972; *Young et al.*, 1977; *Geiss et al.*, 1978; *Horwitz et al.*, 1981, 1983; *Lennartsson et al.*, 1981; *Waite et al.*, 1984] but that the solar activity for the DE 1 data was consistently higher than that for the data from these other studies. *Farrugia et al.* [1989], using data from GEOS, reported a constant He^+ to H^+ ratio of 0.1, also lower than early DE 1/RIMS results. However, *Newberry et al.* [1989], in a comparison of the early DE 1/RIMS data to a physical model, found that the ratio at 5200 km on an L=2 field line should vary with solar and geomagnetic activity. The *Newberry et al.* model results show that He^+ and H^+ have different responses to geomagnetic and solar activity with the effect that the solar input tends to dominate the behavior of the ratio. Although *Newberry et al.* [1989] found that the model consistently produced ratios of order 0.2, it did not reproduce the near constant ratio observed above 4000 km.

With several years of data from DE 1/RIMS now available, covering both high and low solar activity, it seems an advantageous time to examine the low-energy He^+ to H^+ density ratio in more detail; and, in particular, to examine how this ratio varies in the plasmasphere. We do this here using DE 1/RIMS data from the first three and a quarter years of its lifetime, between October 26, 1981, and December 31, 1984, during which the satellite orbit completes a full cycle of precession back to near its original orientation. The data over this time cover the declining phase of the solar cycle from near maximum to minimum, all seasons, and most local times. The same instrument is used for all phases of the solar cycle so that it is possible to follow changes in the ratio with the solar cycle with no instrument cross calibrations. The ratio of He^+ to H^+ density is used rather than the He^+

Copyright 1997 by the American Geophysical Union.

Paper number 96JA02176.
0148-0227/97/96JA-02176$09.00

density itself, in order to check the constancy of this ratio, to avoid having to use separate models for the He^+ and H^+ density, and because in using the ratio, absolute calibrations for each ion are not needed. Since H^+ is the dominant ion above the topside ionosphere, there should be little change in our results if we use the H^+ density rather than the electron density for the total density.

Methods

The RIMS instrument is described in detail by *Chappell et al.* [1981]. There were three RIMS heads on DE 1 and associated with each head was a magnetic mass spectrometer, which had two channel electron multiplier detectors that were placed to simultaneously measure ion species with masses in the ratio of 4 to 1, for example, He^+ and H^+, O^+ and He^+. The ratios in this study all result from simultaneous measurements of He^+ and H^+, He^+ in the high mass channel and H^+ in the low mass channel, from the radial head which looked in a direction perpendicular to the satellite spin axis. Densities are derived from count rate data averaged over a minute (each minute average is referred to as a sample in the following). The satellite orbit limits geocentric distances sampled to 4.5 R_E or less, but the distances at which densities are actually available are limited by the data reduction method.

Densities for each sample (counts) have been derived using a modification of methods described by *Comfort et al.* [1982, 1985], which requires that the ion distribution function be near Maxwellian. Because of a partial failure of the radial head, no energy analysis was available from this head for much of the time covered by the database; however, the radial head did provide the integral count rate, with no retarding. We use the energy analysis available on the two heads pointing parallel and antiparallel to the satellite spin axis to determine the ion species temperatures, according to the method of *Comfort et al.* [1982, 1985], assuming a zero flow velocity to account for the orientation of the detectors transverse to the ram direction. An average of the temperatures from the two heads is used for further processing. With this temperature and the spacecraft velocity, we are able to determine the Mach number of the flow into the radial detector. The effective spacecraft potential is obtained, using the models of *Comfort and Chandler* [1990], from the spin modulation of the radial detector (unretarded) count rate and this Mach number. The peak (unretarded) count rate in the ram direction from the radial head is then used with the temperature and spacecraft potential, as described above, and instrument calibration factors to determine the density according to the method of *Comfort et al.* [1982, 1985].

Temperatures resulting from this method have been compared with those obtained from the radial head when it was fully operational to assure that it provides accurate temperatures. The density calculation in both approaches is based on the peak unretarded count rate of the radial head. It is assumed in this procedure that the ion Maxwellian distribution is isotropic in the plasma frame of reference, and that any flows are small compared with the spacecraft velocity. Also, we analyze only the coldest component observed, as discussed by *Comfort et al.* [1985]. These conditions restrict the observations used to those in and near the plasmasphere [*Comfort et al.*, 1982, 1985].

Because He^+ is taken from the high mass channel and H^+ from the low mass channel, corrections have to be applied to the count rate data to compensate for different sensitivities in the detectors. Since He^+ was paired in the 1 to 4 relation with both H^+ and O^+, anytime these two ions were measured in the same minute, He^+ is obtained in both the high and low mass channel in the same minute. Fortunately, this was the usual mode of operation for RIMS. Consequently, the correction factor, derived from the ratio of the He^+ count rate in the high mass channel to the He^+ count rate in the low mass channel, both count rates separately integrated over the same minute, is a quantitative measure of the relative sensitivities of the high and low mass channel detectors. This ratio varied somewhat from day to day and from measurement to measurement. In order to account for any day-to-day and long-term changes in the relative sensitivities, the correction factor for each data sample is used, excluding from the data set any sample for which there is no corresponding high-low channel correction factor. All available data from 1981 through 1984 are used to find measured correction factors for each sample.

Data taken at high latitudes (Λ>60°), samples with a He^+ to H^+ density ratio greater than 5, and samples for which the measured temperatures of the two ions differ by more than a factor of 2 have been excluded from the data set. The first condition is no practical limitation since there are few derived densities from that region because of the Maxwellian restriction mentioned above. The last two are considered to be nonphysical and reject only a few samples, but ones that are outliers and which, when excluded, reduce the scatter in the results presented here.

We have chosen to use the proxy for the solar EUV devised by *Richards et al.* [1994] as a measure of solar activity. This proxy P is defined as

$$P=(F10.7+F10.7A)/2. \quad (1)$$

where F10.7 is the daily measure of the 10.7 cm solar flux and F10.7A is the 81-day average of the F10.7, with the 81-day average centered on the day of interest. P is a better proxy for the solar EUV, and therefore ion production, than the daily F10.7, particularly at high solar activity [*Richards et al.*, 1994]; it also results in a better separation of the data in terms of high and low solar activity using a single value of P (P=150) for the separation criteria. Figure 1 shows solar activity in terms of the proxy P for the period of this study. Solar activity is seen to be generally high and highly variable in 1981, decaying in both the magnitude and variability into 1984. At the end of 1984, the P values are about 70 with small relative variations (Figure 1). Because of the changing solar cycle, the data for high solar activity (P>150) is concentrated in the early period of DE 1, 1981 into 1983, and low solar activity (P<150) is concentrated in 1983 and 1984.

We use two proxies for geomagnetic activity; one, ΣKp, is the sum of Kp in the previous 24 hours from the time of the measurement. The other, Kp(m) is local time dependent. If the local time of the measurement is between midnight and dusk (0000-1800 hours), Kp(m) is the Kp value at the time the plasma was previously at midnight local time, assuming corotation. If the measurement local time is between dusk and midnight (1800-2400 hours), Kp(m) is the Kp value at the time of the measurement. We use these geomagnetic indices because in one, ΣKp, we get an integrated history and a mea-

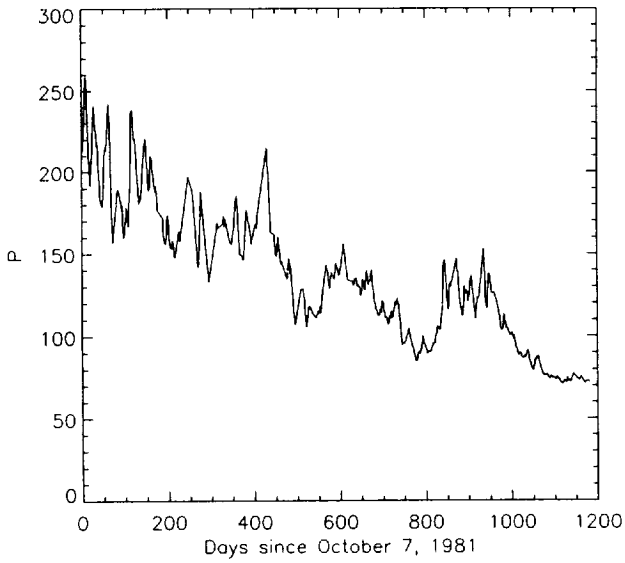

Figure 1. The Richards proxy [*Richards et al.*, 1994] for solar EUV for 1981 to 1984, the time of the DE 1 data used in this report.

sure of the overall level of the geomagnetic activity. The other index, Kp(m), is used in recognition of the influence of conditions near local midnight in determining plasmaspheric conditions at other local times.

We also group the ratios by season. Southern hemisphere summer data are grouped with the northern hemisphere summer data and southern winter data are grouped with northern winter. We do this by shifting the day of year by 180 days if the measurement is in the southern hemisphere and within ±45 days of the solstice. Both fall and spring equinox data are grouped together regardless of hemisphere. There is a relationship between local time and season which is discussed below.

A preliminary examination of the data indicated that the ratio varied most with radial distance r and secondly with solar activity, P. The dependencies on season, local time, geomagnetic activity, and latitude appeared to be much weaker than those with r or with P. However, the spread of the ratios is large, due in part to the variations with r and P. In order to see the weaker dependencies and to model the behavior of the ratio, we detrend the data with respect to the r and P variations. We have used two methods to model the variations of the ratio with r and P. In the first method, the ratio is assumed to be separable into products of functions of each independent variable, that is,

$$R_m^a(r, P, Kp,...) = f(r)g(P)h(Kp)..., \quad (2)$$

where R_m^a is the modeled ratio that incorporates all the known dependencies. This treatment assumes that the independent variables are not correlated, or at least not strongly correlated. Each function was found successively, that is, fit the data to f(r), and remove this trend, then fit this detrended data to g(P) and remove its dependency, and so on. We found through this process, that the r and P dependence of the data could be modeled as the product of exponential functions of r and P, specifically,

$$R_m(r, P) = \exp(a_0+a_1r)\exp(a_2+a_3P+a_4P^2), \quad (3)$$

where now R_m is the modeled ratio that includes only the r and P dependencies. In the second method, rather than finding each function separately, we used multiple linear regression to fit the data with functional forms similar to those used in the separable function method. In performing the multiple regression fit, we also used r, P, and P^2 as the independent variables. P and P^2 are, of course, not independent, but it is necessary to include both in order to model the variation of the density ratio with P. In this second method, the function for the model ratio was actually fit to the log (base 10) of the measured ratio, that is,

$$\log R_m(r,P) = b_0+b_1r+b_2P+b_3P^2. \quad (4)$$

The original data set is detrended for r and P by dividing each measured ratio, R(r, P, Kp,...) by $R_m(r, P)$

$$R_d(Kp,...)=R(r, P, Kp,...) / R_m(r, P), \quad (5)$$

where R_d is the detrended ratio. The two methods yield approximately the same results in terms of R_d, the ratio detrended for r and P, but since the coefficients in the multiple linear regression method are determined simultaneously, this is the method of choice for R_m. The detrended ratios discussed below have been found using the model ratios based on the multiple linear regression fit. The result, R_d, has had the dependency on r and P removed, at least on a statistical basis, leaving the dependencies on the other factors, Kp, local time, season, latitude and L, to be determined. Because these dependencies are non linear, we use polynomials to fit the data to latitude, local time, and L shell. The latitude fit is given by a function of the form

$$R_\lambda = \sum c_n \sinh^n((\lambda+5)\pi / (2\lambda_o)) \quad (6)$$

where $\lambda_o = 60°$. Similarly, the functional form for the fit to local time is given by

$$R_{LT} = \sum d_n \sin^{2n}((LT-2.5)\pi / 24.). \quad (7)$$

The functional form for the fit to the remaining variable, L, is given by

$$R_L = \sum e_n L^n. \quad (8)$$

The final fitted ratio is given by the product of R_m and (6) through (8); the fully detrended ratio R_f is given by

$$R_f = R(r, P, \lambda, LT, L) / (R_m(r,P)R_\lambda R_{LT} R_L) \quad (9)$$

and should show no systematic variation with these variables. We do not use the fits given by (6) through (8) in the discussions below because the variation of the detrended ratio R_d with these variables is small. However, for completeness, the coefficients for our best fits for (6) through (8) are given in Table 1.

Results

In the following, we first examine the results of detrending the He^+ to H^+ density ratio for r and P, and then examine the

Table 1. Coefficients of the Polynomial Equations

	n=0	n=1	n=2	n=3	n=4
Local Time	0.864	1.887	-1.906		
L Shell	-0.298	1.069	-0.315	0.035	
Latitude	0.946	0.043	0.336	-0.169	0.049

characteristics of the detrended ratio as functions of the remaining variables. A statistical approach, as opposed to case studies, is used to determine the basic behavior of the ratio. Temporal characteristics are usually lost in this approach, as are spatial structures and boundaries. However, these features do add to the spread in the data.

Two very basic characteristics of the ratio of He^+ to H^+ densities in the plasmasphere are apparent in this study: the ratio decreases with r in the plasmasphere, and it depends strongly on solar activity. The decrease with r can be seen in Figure 2, which shows the original He^+ to H^+ density ratios as a function of r. All data are included in this plot, a total of 20,338 samples. The trend for the measured ratio R to decrease with geocentric distance is clear, as is the large spread in the ratio for any given geocentric distance. R decreases by approximately an order of magnitude, from about 0.3 to 0.03, between 1 R_E and 4.5 R_E. This decrease of the ratio with geocentric distance is consistent, at least qualitatively, with other studies. Model results of *Angerami and Thomas* [1964] and *Newberry et al.* [1989] show that the ratio decreases with altitude along a field line. In the *Newberry et al.* [1989] study, the ratio decreases from about 1 to about 0.1 between 1000 km altitude and the top of the L=2 field line. The *Angerami and Thomas* [1964] results are for a constant ion temperature of 1500 °K and their He^+ to H^+ density ratio decreases from about 10 at 1000 km to about 0.02 at 8000 km altitude. The ratio as calculated by *Angerami and Thomas* [1964] is temperature dependent and would decrease more slowly with a higher ion temperature. Ratios from GEOS 1 measured densities of H^+ and He^+ near the equatorial plane also indicate that the ratio falls with increasing radial distance [*Farrugia et al.*, 1989]. Our choice of using the radial distance rather than L to examine the ratio is based on our observation that the data is better organized by r than by L. This decision is supported by the smaller linear correlation coefficient associated with L (see Table 2).

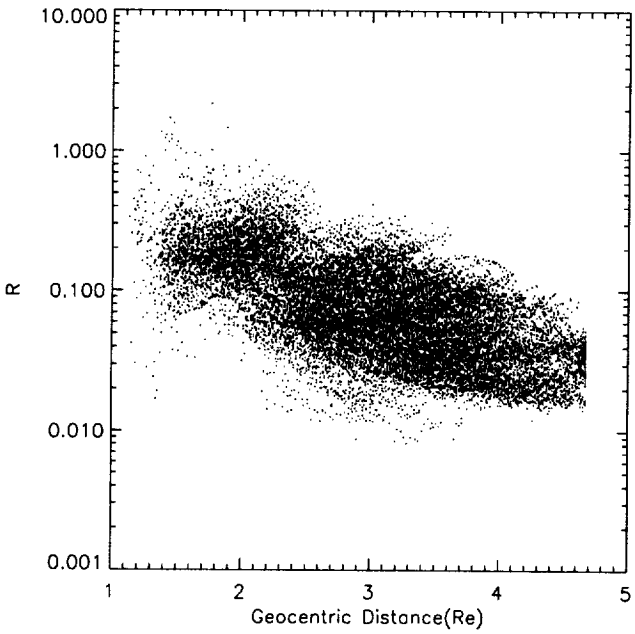

Figure 2. The original He^+ to H^+ ratio plotted as a function of geocentric distance, r (in R_E).

The results of the multiple linear regression fit to the data shown in Figure 2 are given in the first 3 columns of Table 2 in the appendix. The coefficients, b_i, for (4), the linear correlation coefficients, c_l, for each variable as well as the multiple correlation coefficient, C_{mul}, and χ^2 for the overall fit are included in the table. The last two columns in Table 2 show the values of selected coefficients for L and Kp when they are included in the regression. They are shown in Table 2 only for reference since they were not used to detrend the data.

Figure 3 shows the data plotted as a function of r after each point has been detrended according to (5), using (4) and the b_i coefficients given in Table 2. The detrended ratios should cluster around one (the solid line across the graph at one is included for reference) if the trends have been removed. Figure 4 shows the same detrended ratios plotted as a function of P. No dependence on either r or P remains after detrending, and the scatter in the measured density ratios has been reduced.

A third character of the ratio, which is shown in Figure 5 and also by the correlation coefficient given in Table 2, is that there appears to be no correlation between the ratio and geomagnetic activity. The results are the same regardless of which of the two Kp based indices described above are used. *Young et al.* [1982] found little correlation between Kp and the He^+ to H^+ density ratio for higher energy particles(0.9-15.9 keV/e) near geosynchronous orbit (L=6.6). In the Young et al. study, He^+ density is unaffected by Kp and the H^+ density increases by 60 per cent over the full range of Kp so that the ratio decreases by less than 40 percent. Kp (or any other indices related to Kp) may not be a proper proxy to show a relation between the ratio and geomagnetic activity, but this seems unlikely. If the independent variables are correlated, particularly Kp and P, then removal of the dependence of the data on P, would also decrease the variation with Kp. However, we find no correlation between P and Kp over the period of the data set.

The variation of R_d with each of the remaining variables (season, local time, latitude, and L) is small relative to the variation with r or P. The latitudinal dependence of the ratio is presented in Figure 6. R_d appears to maximize near 60° latitude, the maximum occurring near a region traditionally associated with the outer edge of the plasmasphere. Although

Table 2. Coefficients and Correlation Coefficients for the Multiple Linear Regression Fit $b_0 = -1.541$

	r	P	P^2	L	K_p
b_i	−0.176	8.557×10^{-3}	-1.458×10^{-5}		
c_1	−0.648	0.744	0.731	−0.358	0.038
C_{mul}	0.827			0.852	
χ^2	0.036			0.031	

not much variation between ± 40° is seen in Figure 6, the ratio does appear to minimize at the equator for a given pass, at least for the early data; this tendency is not so clear for later measurements.

The orbital precession of DE 1 is such that season and local time are correlated. For this reason, although we examine the behavior of the ratio with both season and local time, we cannot separate the influence of the two parameters. For reference, the intial orbit plane position for the data set (October 26, 1981) corresponds to the 1000 to 2200 magnetic local time longitude. We have chosen to use local time as the variable, but could have used season just as well; the curve fitted to one also follows the data when plotted against the other. The ratio plotted as a function of season (day of year) is shown in Figure 7. The ratio peaks near the equinoxes and minimizes at the solstices, the difference amounting to a factor of about 2. There is a weak systematic variation of the ratio with magnetic local time (see Figure 8). An apparent dip in the ratios near 1500 hours appears to be the result of a concentration of measurements taken close to the same date. The detrended ratios R_d tend to be less than one from about 2200 to about 0500 hour, around one from 0500 to about 0900, and greater than one from 0900 to about 2200 hours, ignoring the dip at about 1500 hours, with the variation being a factor of about 3. The *Newberry et al.* [1989] model results indicate a diurnal variation of a factor of 3-4 in the ratio at 5200 km (the equator at the top of the flux tube) in which the ratio reaches a minimum around 0300 MLT corresponding to a minimum in the He^+ density. The measured data in the Newberry et al. study appear to be consistent with their model results, but none of their observations occur at the local time minimum. *Brinton et al.* [1969] report a diurnal variation in the He^+ to H^+ ratio at about 2700 km and at low latitudes that is similar to the Newberry et al. results, but they show a nearly constant ratio with local time at about 1200 km at midlatitudes. *Bauer* [1966] and *Waite et al.* [1984] note that the ratio is temperature dependent, so that the diurnal variation may decrease on the higher L shells at high altitudes, where the temperatures tend to show little diurnal variation; *Bauer* [1966] suggests that there should be no diurnal variation in the ratio at solar maximum because of the temperature dependence and the higher temperatures. The data shown here are qualitatively consistent with the *Newberry et al.* [1989] results in that the magnitude of the variation is similar and in

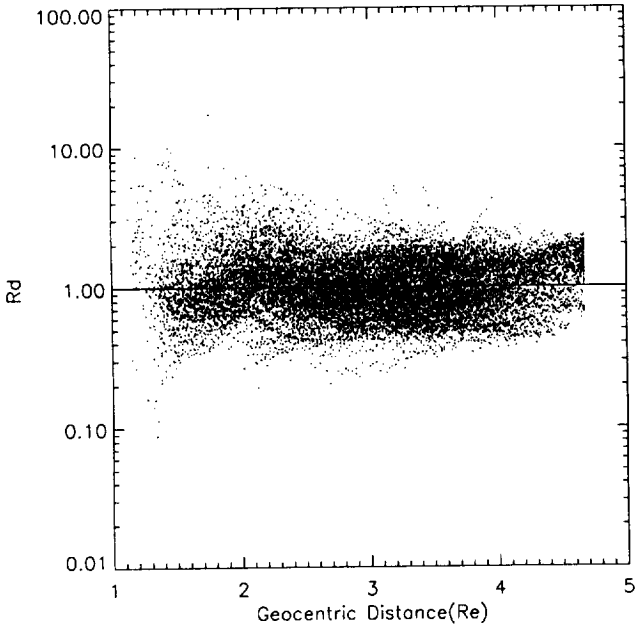

Figure 3. The He^+ to H^+ ratio plotted as a function of r after detrending for both r and P. The line at Rd=1 is drawn for reference only.

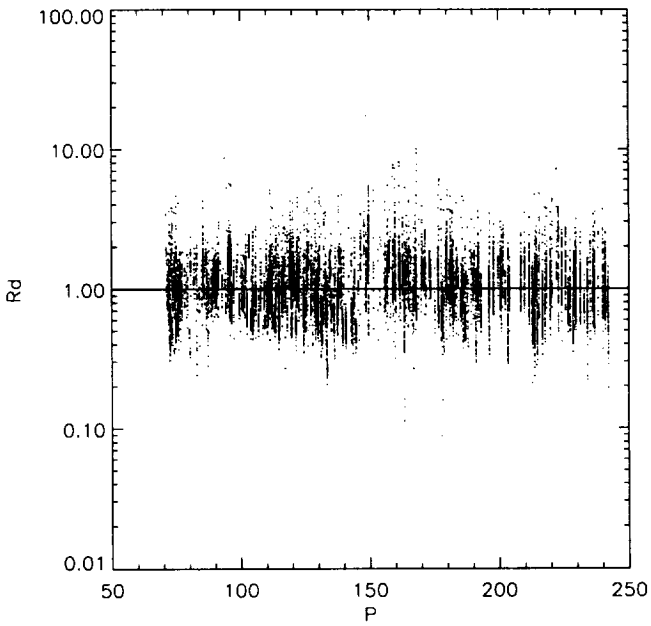

Figure 4. The He^+ to H^+ ratio plotted as a function of P after adjusting for both r and P.

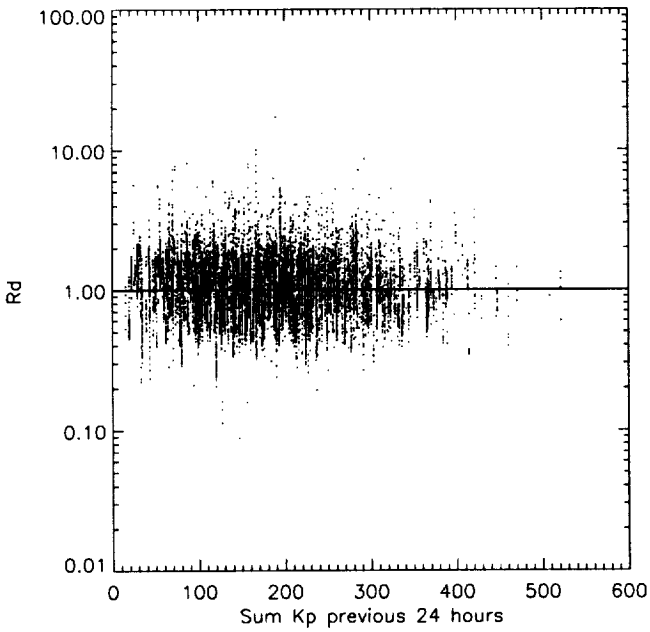

Figure 5. The detrended He^+ to H^+ ratio as a function of the sum of Kp in the 24 hours previous to the time of the measurement.

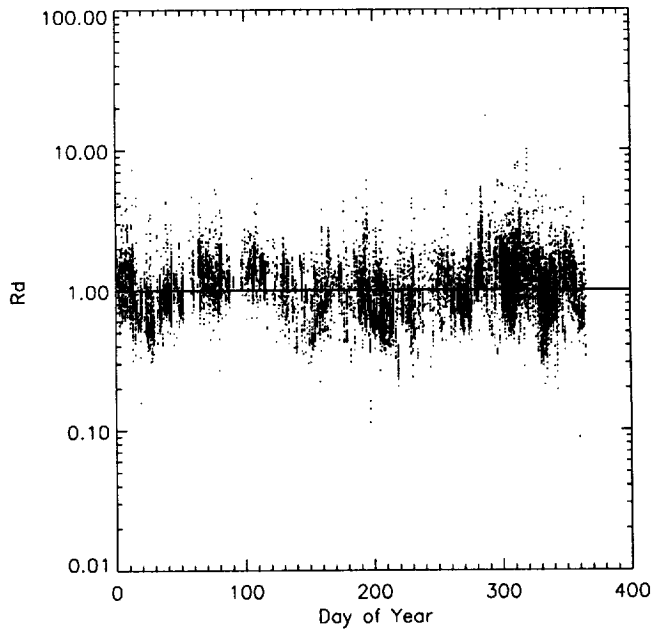

Figure 7. The detrended He^+ to H^+ ratio as a function of the day of the year.

that the ratio is generally smaller in the midnight and dawn hours than during the day.

Discussion

Because the ratios presented here extend over a large number of observations and types of conditions, some spread in the ratios should be expected. The spread in Figure 2 for a given r is greater than a factor of 5, and this variation is on top of a factor of 10 variation between 1 and 4.5 R_E. The total spread is reduced to a factor of 4 to 5 after detrending on r and P, indicating the strong influence of r and P on the ratio. The standard deviation of the data detrended on r and P is 0.57 measured relative to 1.0. After detrending for r, P, latitude, local time(season), and L shell, the standard deviation is reduced to 0.39. Effects contributing to the remaining spread are short term fluctuations in geophysical conditions, experimental uncertainties, and dependencies on geophysical parameters other than those considered here. Since the data in this study are analyzed by an automated

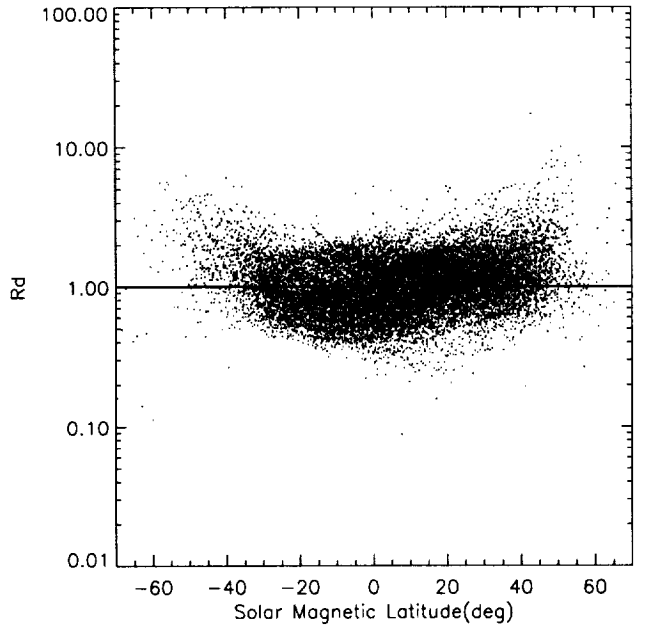

Figure 6. The detrended He^+ to H^+ ratio as a function of latitude.

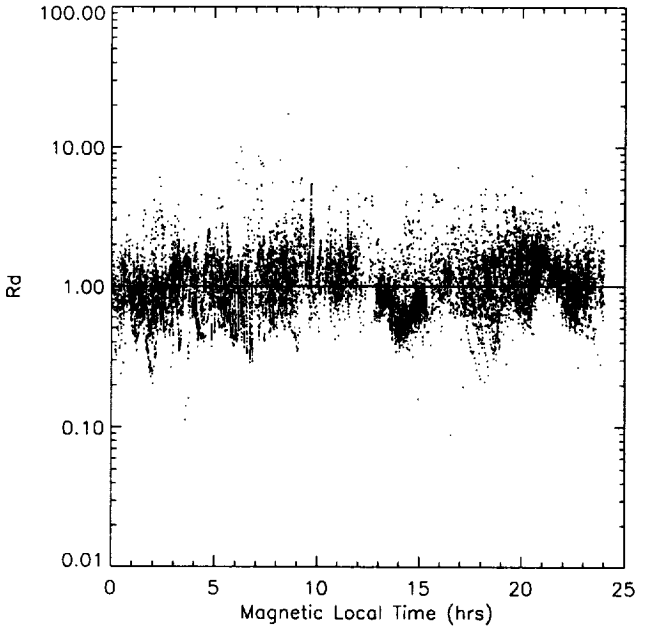

Figure 8. The detrended He^+ to H^+ ratio as a function of magnetic Local Time.

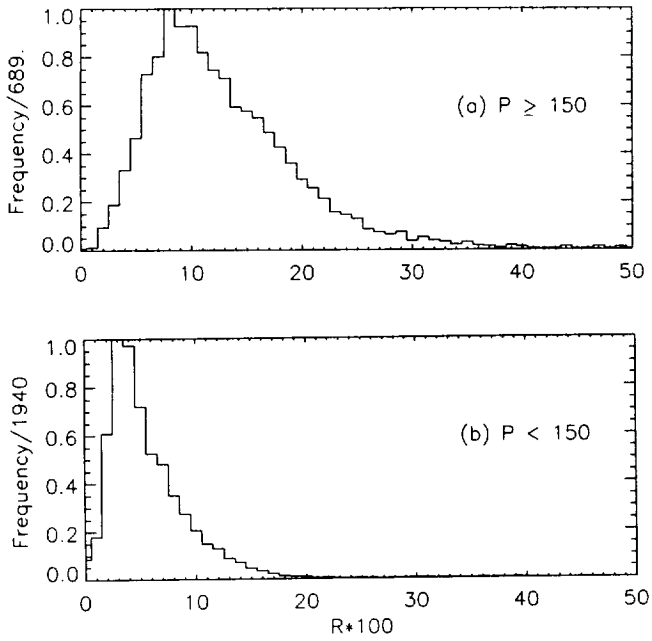

Figure 9. Histograms of the ratio after adjusting for the r dependence and renormalizing to the value at P=150. (a) high solar activity (P≥150) (b) low solar activity (P<150).

system, the "screens" built into the system may allow small deviations from the assumptions on which the method is based; these contribute to the scatter in the data after systematic trends with physical variables have been removed, as described below, but should not be systematic with any geophysical parameters.

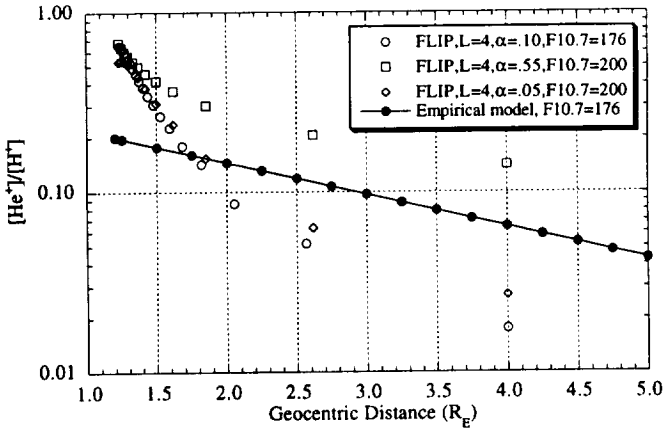

Figure 10. Comparison of results from the physical model (FLIP) with the measured He^+/H^+ ratios. All data are for L=4. The solid line shows the modeled ratio based on the DE 1/RIMS measurements.

A candidate geophysical parameter that may contribute to the remaining spread is the ion temperature. We have looked at the ratio as a function of scale height at the point of the measurement and find the scatter is not reduced by correcting for the point scale height. We assumed that the temperature of the two ions was the same [*Comfort et al.*, 1988; *Farrugia et al.*, 1989; *Comfort*, 1996] and we also ignored the polarization electric field. If the temperature of the ions varies along the field line or if the polarization electric field is included in the treatment, then the ratio at any altitude is the result of the integrated effects of temperature along the field line so that single point temperature considerations are not adequate. In addition, if the polarization electric field is

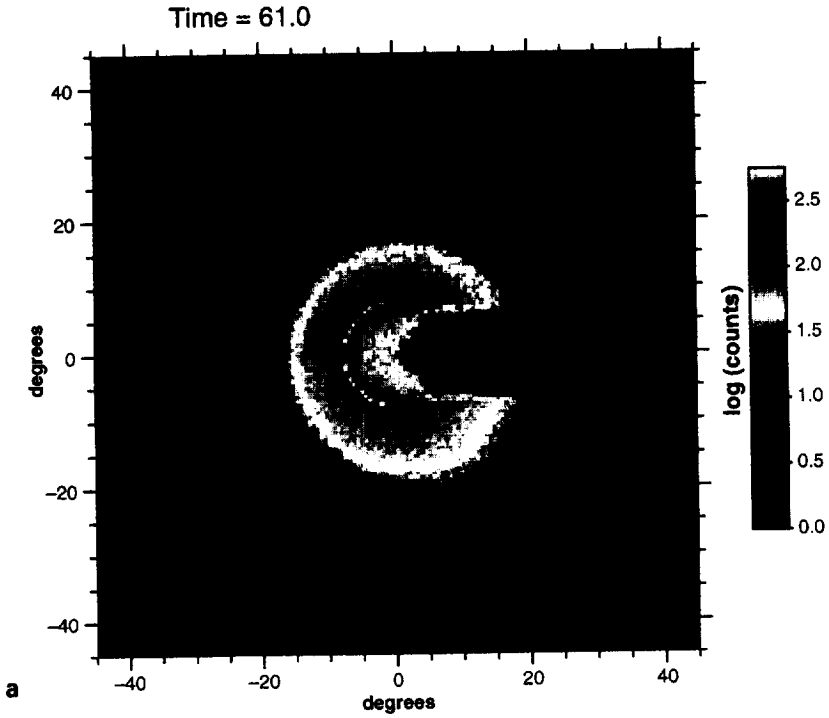

Plate 1. Simulated 304 Å plasmaspheric images (time=61.0). (a) Constant He^+ to H^+ density ratio (0.15), (b) the ratio is a function of r and P, (c) Percentage difference in counts between images in Plate 1a and 1b..

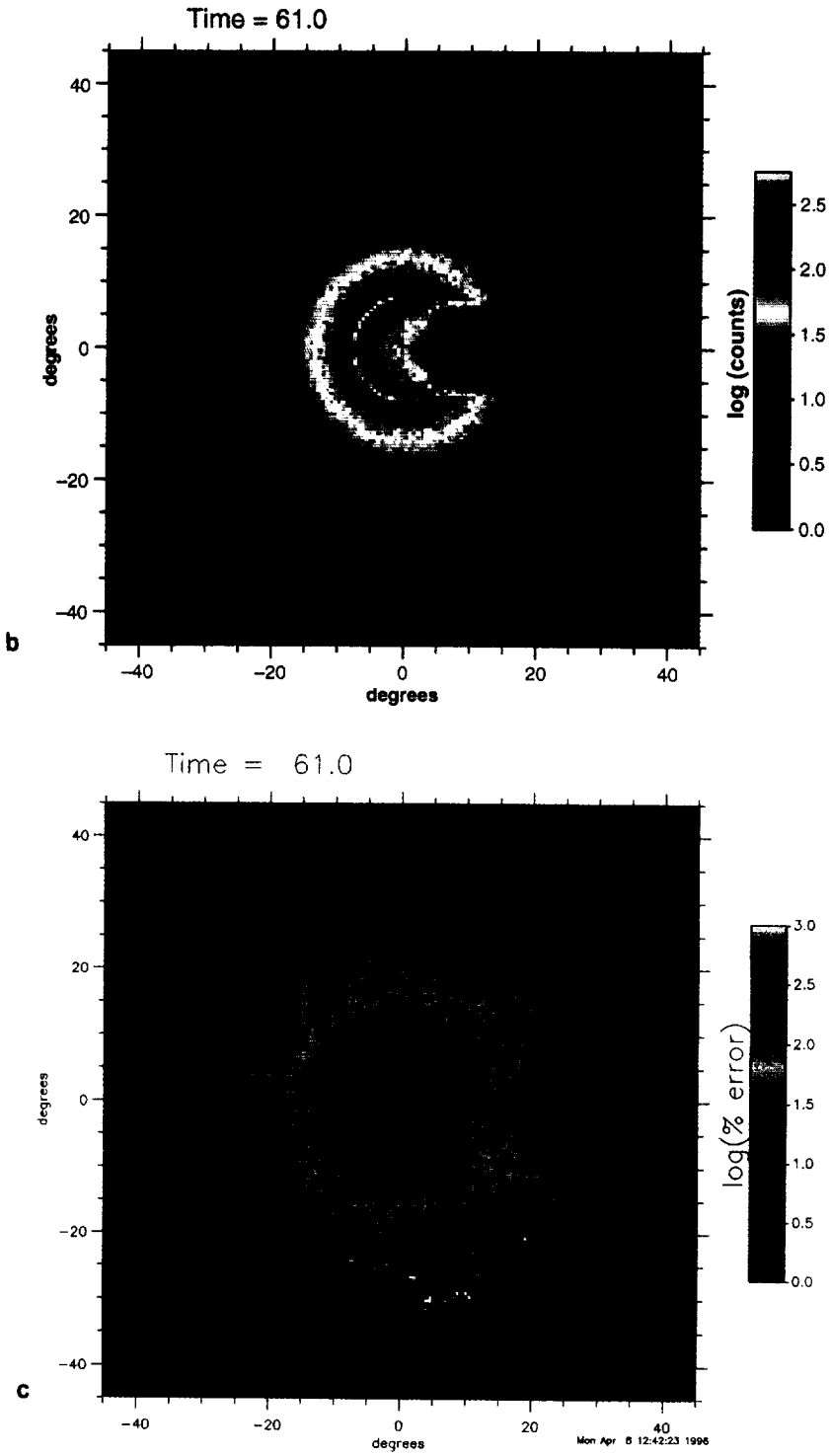

Plate 1. (continued)

included, the ratio of the ion to the electron temperatures is needed [*Angerami and Thomas*, 1964]. That the variation shown in Figure 8 is not a strong function of local time may be related to the effect of the ion temperature on the ratio. Further study along these lines would have to include, at a minimum, an altitude profile of the ion and electron temperatures and their diurnal variation.

Horwitz et al. [1986] noted that the ratio tends to remain constant even across the plasmapause. We also find that ratio changes across the plasmapause, in those cases for which we can track the change (mainly confined to the early data), are much smaller than the spread in the ratios for a given radial distance (see Figure 2), so that transitions across the plasmasphere boundary at midlatitudes to low latitudes do not appear to be adding significantly to this spread. The ratio does appear to systematically increase above ±40° latitude. All the data points near ±60° latitude, the peak of the rise, are at geocentric distances less than 2 R_E. Our detrending for r does not

adjust the ratios in this latitude and altitude range properly, resulting in detrended ratios that are too high. The number of data points at high latitude below 2 R_E is small so that the total contribution to the spread is small and limited to the lower radial distances. The relatively small systematic variations seen in this data with local time, geomagnetic activity, or latitude indicate that changes in the ratio caused by the processes related to these variables are small in comparison to the variations from processes related to r and P.

The importance of determining the variation of the He^+ to H^+ density ratio to the interpretation of images of the plasmasphere should not be overlooked. As noted by *Williams et al.* [1992], in order for images at 304 Å to represent the plasma density and not just He^+ in the plasmasphere, a relationship between He^+ density and the total density must be known. The data presented here suggest that a relationship does exist and can be represented by equations 4 and 5 above. In order to correctly deconvolve images of He^+ scattered 304 Å light and represent the results as total density, this relation must be taken into account. Although H^+ is a close approximation to the total density at altitudes above the transition region (where H^+ and O^+ density are equal), below this altitude, near the topside ionosphere and at lower altitudes, O^+ should properly be included in the approximation to the total plasma density. Very few of the measured ratios presented here are at altitudes at which O^+ is dominant, so we have not included it in this study

Histograms of the He^+ to H^+ density ratios from the DE 1/RIMS data for two levels of solar activity, $P < 150$ and $P \geq 150$, show a dramatic difference in the distributions of the samples which emphasizes the importance of the solar input. For high solar activity, the peak value, after adjusting for the r dependence and normalizing to 0.17 at P=150 to bring the magnitude of the ratio back into its original range, is at 0.08 and there is a broad distribution of values with a mean of 0.14 (Figure 9a). For low solar activity, the peak of the histogram is at 0.03 with a narrow distribution (Figure 9b). The mean adjusted ratio for low activity is 0.07. One of the differences between these two data sets, in addition to the levels of solar activity, is that the variability of the solar proxy P is much greater during the high solar activity than it is during the low activity. Thus it appears that at any given phase of the solar cycle, the range of the He^+ to H^+ density ratios that may be measured and the mean value of the ratio may be connected to the solar variability and to the mean solar activity level, respectively, experienced over the time the data is collected. However, more data, preferably following the ratio through another solar cycle, is needed before a definitive statement can be made. The phase of the solar cycle affects the ratio both through production and loss of He^+ and H^+, through scale height effects related to ion temperature, and through diffusion effects. The latter two are shown in the study by *Waite et al.* [1984], in which they demonstrate the importance of the ion temperature and density ratio at the base of the flux tube to the composition in the plasmasphere.

Previous studies, [*Young et al.*, 1982; *Farrugia et al.*, 1989; *Lennartsson et al.*, 1981, 1982; *Horwitz et al.*, 1986], when taken together, suggest that the He^+ to H^+ density ratio varies with solar activity. The data presented here covering half a solar cycle with a single instrument clearly show the relation of the ratio to the solar cycle and also show that the average tends to about 0.15 for high solar activity and 0.07 for low solar activity, in approximate agreement with these previous studies. The ratios reported by *Comfort et al.* [1988], although plotted as a function of L, are also consistent with the results here, as they should be since that data set is a subset of this one. There is the question of how the ratio can be of order 0.2 , as suggested by early RIMS results [*Horwitz et al.*, 1986], but vary an order of magnitude with r as shown here. The answer to this lies in the fact that the ratio from the early RIMS data is only approximately constant [*Horwitz et al.*, 1986; *Comfort et al.*, 1988] and is taken during a time where the average is about 0.2 due to high solar activity. *Newberry et al.* [1989] and *Comfort et al.* [1988] show that the minimum and maximum mean value of the ratio in the early RIMS data differ by a factor of 2 to 3, depending on whether the morning or evening data are being examined. Early analysis of the DE 1/RIMS data used individual orbital passes of the satellite [*Horwitz et al.*, 1984] or combined several months of data for statistical studies [*Comfort et al.*, 1988]. The variation of the density ratio with geocentric distance was not identified or removed in the previous studies, however the range of the geocentric distances was limited, i.e. generally less than 3 Re. Farrugia et al. [1989] using GEOS/ICE data, did show that the equatorial He^+ to H^+ ratio decreased by a factor of about 2 from 2 Re to 6 Re, a rate somewhat slower than that given here, but still within the spread of the data.

Physical models such as the field line interhemispheric plasma (FLIP) model of *Richards and Torr* [1985], show that in the plasmasphere and for given values of geophysical parameters such as F10.7 and Kp, the He^+ to H^+ density ratio is a function of altitude along the field line, decreasing toward the equator from the topside ionosphere [*Craven et al.*, 1995; *Newberry et al.* 1989]. The ratio should decrease with altitude along L if diffusion is the major process governing the distribution of density along the field line [*Newberry et al.*, 1989] and if H^+ is the dominant ion [*Waite et al.*, 1984]. The behavior of the ratio in the present study (Figure 2) is qualitatively consistent with the results of FLIP as shown in Figure 10. Figure 10 shows the results from the physical model (unfilled symbols) and our empirical model (solid symbols connected by a solid line), both for P=176 and L=4; FLIP results for P=200 are also shown for comparison. A free parameter in the physical model sets additional plasmaspheric heating of ions as a result of the trapping of photoelectrons on field lines and the subsequent loss of their energy to the thermal electrons. From the comparison shown in Figure 10, some additional heating is required in the physical model to keep the helium to hydrogen ion density ratio at the measured levels for radial distances larger than 2 R_E. Comparison of the two plots for F10.7=200 in Figure 10 shows the effect of the ion temperature on the altitude profile of the ratio. It is clear that significant additional heat is needed in the physical model in order to slow the decrease of the density with radial distance. A possible source of this heat in the outer plasmasphere may be related to interactions at the equator with ring current plasma [*Fok et al.*, 1996]. The differences between the measured and modeled ratios for $1. < r/R_E \leq 2.$ are not entirely understood. Differences in the model and measured density of He^+ have previously been noted by *Craven et al.* [1995] and *Bailey and Sellek* [1989].

Quantitative agreement between physical models and the DE 1/RIMS data can be checked on a case by case basis or by

averaging the data and comparing with representative model runs covering a variety of conditions (solar activity, geomagnetic activity, time of year, etc.). Only a limited number of the latter have been done, for example, *Newberry et al.* [1989], but good agreement between measurement and theory was obtained. This was also the case in a comparison between data from the Atmospheric Explorers and the FLIP model [*Craven et al.*, 1995], but it was also shown in that study that the treatment of He^+ in the physical models may need to be revised in order to obtain better agreement with measurements. A more complete examination of the different contributions to the He^+ and H^+ densities is needed in order to explain observed He^+ to H^+ density ratios; that will be addressed in a future study.

As a demonstration of the use of our result for the He^+ to H^+ density ratio, we compare simulated images of the magnetosphere in 304 Å scattered radiation using our model to simulated images with a constant He^+ to H^+ density ratio (He^+/H^+=0.15). In both simulations, we use a total density model which is based on the model of *Rasmussen and Schunk* [1990]. We used each model of the density ratio to obtain simulated images of the magnetosphere in 304 Å scattered solar radiation in terms of counts per sample into a instrument and these are shown in Plate 1, Plate 1a for the constant density model and Plate 1b for our model. In each of these simulated images, the view is from above the pole looking down on the Earth, with the Sun to the left, opposite the shadow. The important point is the difference between them, since the only difference in the simulation is the distribution of the He^+. The quantitative differences are shown in Plate 1c. In this panel we show the percentage difference (error) of the counts between the two images. There is at least a factor of 2 difference in the counts on the outer edge of the plasmasphere between the two models with the difference going as high as a factor of 10 in some places. There are also significant differences in the inner regions. The differences seen in Plate 1c could affect the design and operation of an imaging instrument and the interpretation of 304 Å plasmaspheric images.

Conclusions

We have shown through a statistical study, that the observed He^+ to H^+ ratios decrease with geocentric distance (or altitude) and that the decrease is about an order of magnitude between about 1 R_E and 4.5 R_E. Although it has been suggested by physical models that the ratio should decrease with altitude along a field line, until now it has not been demonstrated with observations how this behavior relates to radial distance. We also show that the ratio increases nonlinearly with solar activity. The variation of the ratio with the solar cycle is significant, being about a factor 5 greater for higher activity than for low. Taking into account the distance and solar activity dependence, the ratio has no apparent dependence on geomagnetic activity and is weakly dependent on latitude, L shell, and with one or both of the parameters local time and seasons (we cannot separate the influence of these two with DE 1/RIMS data alone). It is clear from the *Newberry et al.* [1989] study, the study of *Young et al.* [1982], and this study that any dependence of the density ratio on Kp is much weaker than the dependence on P. The cause of the remaining spread in the ratio for any given value of an independent variable is unknown. Studies to determine the causative processes of the remaining spread will need to consider geomagnetic activity history, ion temperatures, and production of He^+ and H^+ in the ionosphere. We show through simulated images of the magnetosphere, that the signal received in 304 Å scattered solar radiation with our model is significantly different from that obtained with a constant density model. Such differences would affect such things as the integration time in the planning and operation phase of an imaging mission and also the inferred density from an image. Missions that image the magnetosphere in 304 Å solar radiation will need to use a model of the He^+ distribution, preferably one based on observation such as we provide here, to help interpret the images.

Acknowledgment. The authors gratefully acknowledge the support of T. E. Moore and members and the RIMS team, particularly B. Giles who helped make the data available to us. We thank the referees for their helpful suggestions and comments. The work of RHC was partially supported under NASA grant NCC8-65 with UAH. This research was also supported by the Office of Space Sciences at the National Aeronautics and Space Administration.

The Editor thanks C. J. Farrugia and S. A. Fuselier for their assistance in evaluating this paper.

References

Angerami, J. J., and J. O. Thomas, Studies of planetary atmospheres 1. The distribution of electrons and ions in the Earth's exosphere, *J. Geophys. Res.*, *69*, 4537, 1964.

Bailey, G. J., and R. Sellek, A mathematical model of the Earth's plasmasphere and its application in a study of He^+ at L=3, *Ann. Geophys.*, *8*, 171, 1989.

Bauer, S. J., Hydrogen and helium ions, *Ann. de Geophys. 22*, 247, 1966.

Bilitza, D., K. Rawer, L. Bossy, and T. Gulyaeva, International Reference Ionosphere- Past , present, and future: II. Plasma temperatures, ion composition, and ion drift, *Adv. Space Res.*, 13(9) 15, 1993.

Brinton, H. C., R. A. Pickett, and H. A. Taylor, Diurnal and seasonal variation of atmospheric ion composition; Correlation with solar zenith angle, *J. Geophys. Res.*, *74*, 4064, 1969.

Carpenter, D. L., and R. R. Anderson, An ISEE/Whistler model of the equatorial electron density in the magnetosphere, *J. Geophys. Res.*, *97*, 1097, 1992.

Chappell, C. R., Recent satellite measurements of the morphology and dynamics of the plasmasphere, *Rev. Geophys.*, *10*, 951-979, 1972.

Chappell, C. R., S. A. Fields, C. R. Baugher, J. H. Hoffman, W. B. Hanson, W. W. Wright, H. D. Hammack, G. R. Carigen, and A. F. Nagy, The retarding ion mass spectrometer on Dynamics Explorer-A, *Space Sci. Instrum.*, *5*, 477, 1981.

Comfort, R. H., and M. O. Chandler, Semiempirical analytical model for the spin modulation of retarding potential analyzer fluxes, *J. Spacecraft*, 27(6), 577, 1990.

Comfort, R. H., Thermal structure of the plasmapause, *Adv. Space Res.*, *17*, (10)175, 1996.

Comfort, R. H., C. R. Baugher, and C. R. Chappell, Use of the thin sheath approximation for obtaining ion temperatures from the ISEE 1 limited aperture RPA, *J. Geophys. Res.*, *87*, 5109, 1982.

Comfort, R. H., J. H. Waite Jr., and C. R. Chappell, Thermal ion temperatures from the retarding ion mass spectrometer on DE 1, *J. Geophys. Res.*, *90*, 3475, 1985.

Comfort, R. H., I. T. Newberry, and C. R. Chappell, Preliminary statistical survey of plasmaspheric ion properties from observations by DE 1/RIMS, in *Modeling Magnetosphere Plasma, Geophys. Monogr. Ser.*, vol. 44, edited by T. E. Moore and J. H. Waite Jr., pp. 107-114, AGU, Washington, D.C., 1988.

Comfort, R. H., P. G. Richards, P. D. Craven, and M. O. Chandler, Problems in simulating ion temperatures in low density flux tubes, in

Cross-Scale Coupling in Space Plasmas, Geophys. Monogr. Ser., vol. 93, edited by J. L. Horwitz, N. Singh, and J. L. Burch, pp. 155-160, AGU, Washington, D.C., 1996.

Craven, P. D., R. H. Comfort, D. L. Gallagher, and R. West, A study of the statistical behavior of ion temperatures from DE 1/ RIMS, in *Modeling Magnetospheric Plasma Processes, Geophys. Monogr. Ser.*, vol. 62, edited by G. R. Wilson, pp. 173-182,AGU, Washington, D.C., 1991.

Craven, P. D., R. H. Comfort, P. G. Richards, and J. M. Grebowsky, Comparisons of modeled N^+, O^+, H^+, and He^+ in the midlatitude ionosphere with mean densities and temperatures from Atmosphere Explorer, *J. Geophys. Res.*, *100*, 257, 1995.

Farrugia, C. J., D. T. Young, J. Geiss, and H. Balsiger, The composition, temperature, and density of cold ions in the quite terrestrial plasmasphere: GEOS 1 results, *J. Geophys. Res.*, *94*, 11,865, 1989.

Fok, M. C., P. D. Craven, T. E. Moore, and P. G. Richards, Ring current-plasmasphere coupling through Coulomb collision, in *Cross-Scale Coupling in Space Plasmas. Geophys. Monogr. Ser.*, vol. 93, edited by J. L. Horwitz, N. Singh, and J. L. Burch, pp. 161-171, AGU, Washington, D.C., 1996.

Geiss, J., H. Balsiger, P. Eberhart, H. P. Walker, L. Weber, and D. T. Young, Dynamics of magnetospheric ion composition as observed by the GEOS mass spectrometer, *Space Sci. Rev.*, *22*, 537, 1978.

Horwitz, J. L., C. R. Baugher, C. R. Chappell, E. G. Shelley, D. T. Young, and R. R. Anderson, ISEE 1 observations of thermal Plasma in the vicinity of the plasmasphere during periods of quieting magnetic activity, *J. Geophys. Res.*, *86*, 9989, 1981.

Horwitz, J. L., C. R. Chappell, D. L. Reasoner, P. D. Craven, J. L. Green, and C. R. Baugher, Observations of low-energy plasma composition from the ISEE 1 and SCATHA satellites, in *Energetic Ion Composition in the Magnetosphere*, edited by R. G. Johnson, pp. 263-268, Terra, Tokyo, 1983.

Horwitz, J. L., R. H. Comfort, and C. R. Chappell, Thermal ion composition measurements of the formation of new outer plasmasphere and double plasmapause during storm recovery phase, *Geophys. Res. Lett.*, *11*, 701, 1984.

Horwitz, J. L., L. H. Brace, R. H. Comfort, and C. R. Chappell, Dual spacecraft measurements of plasmasphere-ionosphere coupling, *J. Geophys. Res.*, *91*, 11203, 1986.

Johnson, C. Y., J. M. Young, and J. C. Holmes, Magnetoglow—A new geophysical resource, *Science*, *171*, 379, 1971.

Lennartsson, W., R. D. Sharp, E. G. Shelley, R. G. Johnson, and H. Balsiger, Ion composition and energy distribution during 10 magnetic storms, *J. Geophys. Res.*, *86*, 4628, 1981.

Lennartsson, W., and R. D. Sharp, A comparison of the 0.1-17 keV/e ion composition in the near equatorial magnetosphere between quiet and disturbed conditions, *J. Geophys., Res.*, *87*, 6109, 1982.

Meier, R. R., Ultraviolet spectroscopy and remote sensing of the upper atmosphere, *Space Sci. Rev.*, *59*, 1, 1991.

Meier, R. R., and C. S. Weller, EUV resonance radiation from helium atoms and ions in the geocorona, *J. Geophys. Res.*, *77*, 1190, 1972.

Newberry, I. T., R. H. Comfort, P. G. Richards, and C. R. Chappell, Thermal He^+ in the plasmasphere: Comparison of observations with numerical calculations, *J. Geophys. Res.*, *94*, 15265, 1989.

Rasmussen, C. E., and R. W. Schunk, A three-dimensional time-dependent model of the Plasmasphere, *J. Geophys. Res.*, *95*, 6133, 1990.

Richards, P. G., and D. G. Torr, Seasonal diurnal and solar cyclical variations of the limiting H^+ flux in the Earth's topside ionosphere, *J. Geophys. Res.*, *90*, 5261, 1985.

Richards, P. G., J. A. Fennelly, and D. G. Torr, EUVAC: A solar EUV flux model for aeronomic calculations, *J. Geophys. Res.*, *99*, 8981, 1994.

Waite, J. H., Jr., J. L. Horwitz, and R. H. Comfort, Diffusive equilibrium distributions of He^+ in the plasmasphere, *Planet. Space. Sci.*, *52*, 611, 1984.

Weller, C. S., and R. R. Meier, First satellite observations of the He^+ 304 Å radiation and its interpretation, *J. Geophys. Res.*, *79*, 1572, 1974.

Williams, D. J., E. C. Roelof, and D. G. Mitchell, Global magnetospheric imaging, *Rev. Geophys.*, *30*, 183, 1992.

Young, D. T., J. Geiss, H. Balsiger, P. Eberhart, A. Ghielmetti, and H. Rosenbauer, Discovery of He^{++} and O^{++} ions of terrestrial origin in the outer magnetosphere, *Geophys. Res. Lett.*, *4*, 561, 1977.

Young, D. T., H. Balsiger, and J. Geiss, Correlations of magnetospheric ion composition with geomagnetic and solar activity, *J. Geophys. Res.*, *87*, 9077, 1982.

P.D. Craven and D.L. Gallagher, Space Sciences Laboratory, NASA Marshall Space Flight Center, Huntsville, AL 35812. (e-mail: craven@msfc.nasa.gov)

R.H. Comfort, Center for Space Plasma and Aeronomic Research, University of Alabama in Huntsville, AL 35899.

(Received November 6, 1995; revised July 8, 1996; accepted July 9, 1996.)